# Analytical study of optical bistability in silicon ring resonators

**Ivan D. Rukhlenko,[1,*] Malin Premaratne,[1] and Govind P. Agrawal[2]**

[1]*Advanced Computing and Simulation Laboratory, Monash University, Clayton, Victoria 3800, Australia*
[2]*The Institute of Optics, University of Rochester, Rochester, New York 14627, USA*
**Corresponding author: ivan.rukhlenko@eng.monash.edu.au*

Received October 14, 2009; revised November 22, 2009; accepted November 23, 2009;
posted December 8, 2009 (Doc. ID 118564); published December 24, 2009

We analyze theoretically the nonlinear phenomenon of optical bistability inside a ring resonator formed with a silicon-waveguide nanowire and derive an exact parametric relation connecting the output intensity to the input intensity. Our input–output relation accounts for linear losses, the Kerr nonlinearity, two-photon absorption, free-carrier-induced absorption and dispersion, and thermo-optic effects within the resonator. Based on our study, we generalize the standard definition of effective length to allow for all possible losses within a silicon ring resonator. We also present a simplified version of the bistable phenomenon valid for resonators operating in a regime in which losses resulting from two-photon absorption are relatively small. Our analytical results provide clear insight into the physics behind optical bistability and may be useful for designing silicon-based optical memories. 

*OCIS codes:* 190.1450, 040.6040, 250.4390, 230.4320, 140.4780, 250.6715.

Owing to their natural compatibility with the existing silicon-based microelectronics technology, silicon-on-insulator (SOI) waveguides are considered to be a potential candidate for future photonic integrated circuits [1,2]. In contrast with optical fibers, SOI waveguides not only allow one to effectively guide light in submicrometer dimensions, but they also possess a number of practically useful optical properties that are lacking in fused silica. Specifically, near the telecommunication wavelength of 1.55 $\mu$m, silicon exhibits considerable two-photon absorption (TPA). Resulting TPA-generated free electrons and holes lead to free-carrier absorption (FCA), free-carrier dispersion (FCD), and the thermo-optic effect (TOE). It has been shown experimentally that these effects are important for the nonlinear phenomenon of optical bistability and govern the input–output characteristics of SOI waveguide resonators [3–7]. However, engineering silicon resonators for nanoscale applications will require a unified analytical theory of optical bistability that takes into account all these effects simultaneously. Recently, we have developed such a theory to describe the bistable operation of a Fabry–Perot resonator in the cw regime [8]. In this Letter, for the first time to the best of our knowledge, we present a similar analytical model for optical bistability in a ring resonator.

Consider a cw signal at an angular frequency $\omega$ propagating inside a straight SOI waveguide coupled laterally to a silicon ring of radius $R$, as shown in Fig. 1. The evolution of electric field $E(z)$ associated with this optical wave is described by a nonlinear differential equation [2,9]

$$\frac{1}{A}\frac{\mathrm{d}A}{\mathrm{d}z} = -\frac{\alpha}{2} - \left(\frac{\beta}{2} - i\gamma\right)|A|^2 - \left(\frac{\xi_r}{2} + i\xi_i\right)|A|^4, \quad (1)$$

where $A(z)$ is the complex amplitude (with $|A|^2$ representing intensity) related to the electric field as $E(z)=\varpi A(z)\exp(i\beta_0 z)$; $\varpi=(\mu_0/\epsilon_0)^{1/4}(2n_0)^{1/2}$; $\mu_0$ and $\epsilon_0$ are, respectively, the intrinsic permeability and permittivity of vacuum; $n_0$ is the linear refractive index, $\beta_0=n_0k$ is the propagation constant with $k=\omega/c$; and $c$ is the speed of light in vacuum.

The parameters entering Eq. (1) are as follows: $\alpha$, $\beta$, and $\gamma=kn_2$ govern, respectively, linear losses, TPA, and the Kerr effect, $n_2$ being the nonlinear Kerr parameter. The parameters $\xi_r$ and $\xi_i$ account for the free-carrier effects and are defined as

$$\xi_r = \sigma\tau\beta/(2\hbar\omega), \quad \xi_i = (\mu/2)\xi_r, \quad \mu = 2k\sigma_n/\sigma_r,$$

where $\sigma=\sigma_r(\omega_r/\omega)^2$, $\sigma_r=1.45\times10^{-21}$ m$^2$, $2\pi c/\omega_r=1.55$ $\mu$m, $\sigma_n=5.3\times10^{-27}$ m$^3$, and $\tau$ is the effective free-carrier lifetime [2]. Even though the TOE is not accounted for in Eq. (1), it can be easily introduced by the replacement of $\mu$ with $\mu'=\mu-2k\beta\kappa\vartheta/(\xi_rC\rho)$, where $\kappa$, $\theta$, $C$, and $\rho$ are, respectively, the thermo-optic coefficient, thermal dissipation time, thermal capacity, and density of silicon [8].

A general theoretical analysis of optical bistability in silicon resonators is possible because Eq. (1) can be solved analytically. However, before addressing the general problem, we consider a practically important case in which the impact of TPA on the attenuation of optical wave is relatively small compared with other

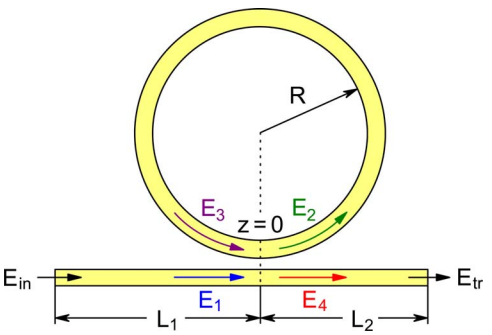


Fig. 1. (Color online) Schematic of the silicon ring resonator and details of the notation employed.

0146-9592/10/010055-3/$15.00 

loss sources. It can be easily shown that this scenario is realized in resonators with $\alpha\xi_r \gg \beta^2$. Seeking the solution of Eq. (1) with $\beta=0$ in the form $A(z)=\sqrt{I(z)}\exp[i\phi(z)]$, we find

$$I(z)=\frac{I_0\exp(-\alpha z)}{\sqrt{1+I_0^2(\xi_r/\alpha)[1-\exp(-2\alpha z)]}}, \tag{2a}$$

$$\phi(z)=\phi_0+\gamma I_0 L_{\mathrm{eff}}(z)-\frac{\xi_i}{\xi_r}\left(\ln\frac{I_0}{I(z)}-\alpha z\right), \tag{2b}$$

where $I_0$ and $\phi_0$ are the values of intensity and phase at $z=0$, and the generalized effective length is given by [10]

$$L_{\mathrm{eff}}(z)=\frac{\tan^{-1}[I_0\sqrt{\xi_r/\alpha}]-\tan^{-1}[I(z)\sqrt{\xi_r/\alpha}]}{I_0\sqrt{\alpha\xi_r}}. \tag{3}$$

These equations describe evolution of the electric field along both the straight and ring waveguides in Fig. 1.

To find transmittance of the ring resonator, we assume that the coupling between optical waves propagating in the ring and straight waveguide is lumped at one point $z=0$ (see Fig. 1). Then the electric fields on both sides of the point coupler satisfy the relations [11]

$$E_4=rE_1+itE_3,\quad E_2=itE_1+rE_3, \tag{4}$$

where $t=\sqrt{1-r^2}$, and $r^2$ is the fraction of power remaining in the straight waveguide after the coupler. Eliminating $E_1$ from Eqs. (4) and noting that $E_2=E(0)$ and $E_3=E(2\pi R)$, we can express the intensity $I_4=|E_4|^2/\varpi^2$ in terms of $I_0=|E_2|^2/\varpi^2$ as

$$I_4(I_0)=\frac{r^2I_0+I(2\pi R)-2r\sqrt{I_0I(2\pi R)}\cos\Delta\phi}{1-r^2}, \tag{5}$$

where $\Delta\phi=2\pi\beta_0R+\phi(2\pi R)-\phi_0$ is the phase shift acquired during one round trip within the ring. A similar relation for the intensity $I_1=|E_1|^2/\varpi^2$ can be deduced from the energy conservation law and is given by

$$I_1(I_0)=I_0-I(2\pi R)+I_4(I_0). \tag{6}$$

If $L_1$ and $L_2$ are lengths of the straight waveguide before and after the coupling point (see Fig. 1), the intensities at the input and output ends of the straight waveguide can be related to $I_1$ and $I_4$ by

$$I_{\mathrm{in}}(I_0)=\frac{I_1(I_0)\exp(\alpha L_1)}{\sqrt{1+I_1^2(I_0)(\xi_r/\alpha)[1-\exp(2\alpha L_1)]}}, \tag{7a}$$

$$I_{\mathrm{tr}}(I_0)=\frac{I_4(I_0)\exp(-\alpha L_2)}{\sqrt{1+I_4^2(I_0)(\xi_r/\alpha)[1-\exp(-2\alpha L_2)]}}. \tag{7b}$$

Substituting Eqs. (2), (5), and (6) into Eqs. (7), we obtain in a parametric form the input–output relation $I_{\mathrm{tr}}(I_{\mathrm{in}})$ of the silicon ring resonator. However, to use it, we first need to find the set of values that $I_0$ can acquire for a given input intensity.

Because of the periodic nature of the relation in Eq. (5), $I_0$ can have multiple values for a given value of $I_{\mathrm{in}}$. It is easy to deduce from Eq. (7a) that, in the limit $I_{\mathrm{in}}\to\infty$, the value of $I_1$ is given by the simple relation

$$I_1(\mathfrak{I})=\left(\frac{\alpha/\xi_r}{\exp(2\alpha L_1)-1}\right)^{1/2}. \tag{8}$$

The parameter $I_0$ can thus lie in the intervals $[0,\mathfrak{I}_1)$, $(\mathfrak{I}_2,\mathfrak{I}_3),\ldots,(\mathfrak{I}_{n-1},\mathfrak{I}_n)$, where $\mathfrak{I}_j$ $(j=1,\ldots,n)$ are the roots of the preceding transcendental equation. Assuming that $L_1\neq 0$ or $L_2\neq 0$, the bistability described by Eqs. (7) exhibits a saturable character owing to the presence of FCA. The maximum limiting output intensity in the FCA-induced saturation regime is given by $I_{\max}\equiv I_{\mathrm{tr}}(\mathfrak{I}_1)$.

When TPA contribution cannot be ignored, an exact solution of Eq. (1) is required. After some algebra, we were able to solve it in the following implicit form:

$$2\alpha z+\beta I_0\mathcal{L}_{\mathrm{eff}}(z)=\ln\frac{\alpha I^{-2}(z)+\beta I^{-1}(z)+\xi_r}{\alpha I_0^{-2}+\beta I_0^{-1}+\xi_r}, \tag{9a}$$

$$\phi(z)=\phi_0+\gamma I_0\mathcal{L}_{\mathrm{eff}}(z)-\frac{\xi_i}{\xi_r}\left[\ln\frac{I_0}{I(z)}-\alpha z-\frac{\beta}{2\gamma}\mathcal{L}_{\mathrm{eff}}(z)\right], \tag{9b}$$

where

$$\mathcal{L}_{\mathrm{eff}}(z)=\frac{q}{\beta I_0}\ln\left[\frac{qK(z)+1}{qK(z)-1}\frac{qK(0)-1}{qK(0)+1}\right], \tag{10}$$

$q=(1-4\alpha\xi_r/\beta^2)^{-1/2}$, and $K(z)=1+2(\xi_r/\beta)I(z)$. This solution is valid irrespective of whether $q$ is real or imaginary. Since $\mathcal{L}_{\mathrm{eff}}(z)\to L_{\mathrm{eff}}(z)$ as $\beta\to 0$, Eq. (10) can be considered a generalization of the effective length given in Eq. (3) to the case of non-negligible TPA.

If we denote by $I(I_0,z)$ the solution of Eq. (9a), the evolution of transmitted intensity with the input intensity in the presence of TPA can be written in the parametric form

$$I_{\mathrm{in}}(I_0)=I[I_1(I_0),-L_1],\quad I_{\mathrm{tr}}(I_0)=I[I_4(I_0),L_2], \tag{11}$$

where $I_0$ again lies in the intervals $[0,\mathcal{I}_1)$, $(\mathcal{I}_2,\mathcal{I}_3),\ldots,(\mathcal{I}_{n-1},\mathcal{I}_n)$, but now $\mathcal{I}_j$ with $j=1,\ldots,n$ are the roots of the new transcendental equation

$$\frac{\xi_rI_1^2(\mathcal{I})\exp(2\alpha L_1)}{\alpha+\beta I_1(\mathcal{I})+\xi_rI_1^2(\mathcal{I})}=\left(\frac{\chi(\mathcal{I})-1}{\chi(\mathcal{I})+1}\right)^q \tag{12}$$

with $\chi(\mathcal{I})=q[1+2(\xi_r/\beta)I_1(\mathcal{I})]$. In Eqs. (11) and (12), functions $I_1(I_0)$ and $I_2(I_0)$ are given by Eqs. (5) and (6), provided that the solution $I(I_0,2\pi R)$ of Eq. (9a) is used there. The maximum limiting output intensity in the presence of TPA is given by $I_{\max}\equiv I_{\mathrm{tr}}(\mathcal{I}_1)$.

To illustrate the bistable behavior, we focus on a silicon ring resonator with 5 $\mu$m radius and set $L_1=L_2=10$ $\mu$m, $r=0.1$, $n_0=3.484$, $\alpha=1$ dB/cm, $\beta=0.5$ cm/GW, and $n_2=6\times10^{-5}$ cm$^2$/GW. Figure 2

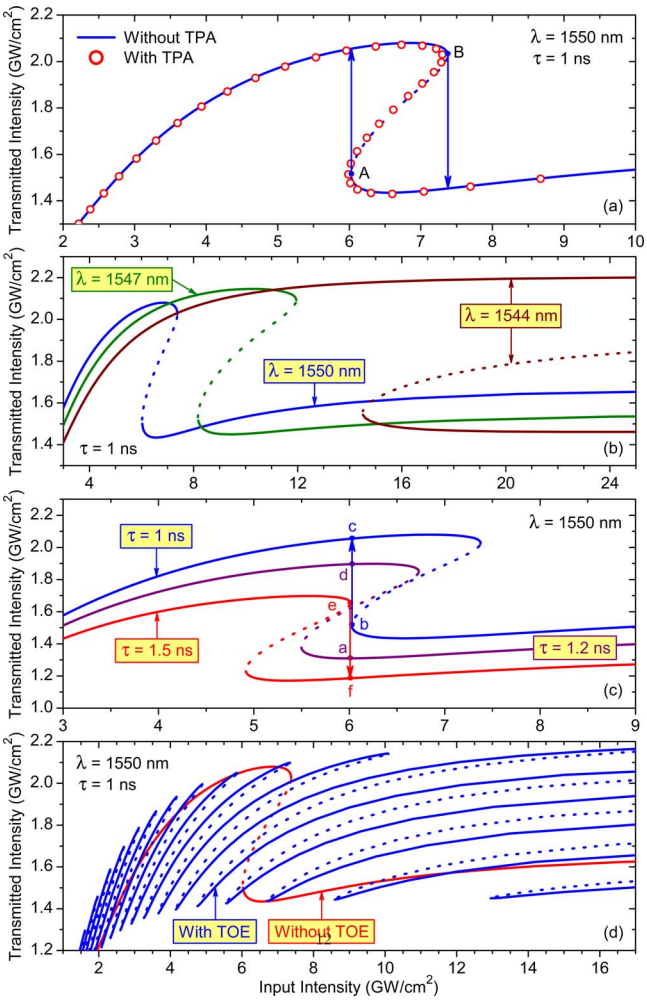


Fig. 2. (Color online) Bistable characteristics of a silicon ring resonator of 5 $\mu$m radius: (a) comparison between approximate (solid curve) and exact (open circles) solutions; (b) bistable curves at three operating wavelengths; (c) electronically assisted optical switching at a fixed input intensity; and (d) the impact of the thermo-optic effect (TOE) on optical bistability. TOE is absent in panels (a)–(c).

shows the bistability curves in different operation regimes of such resonator. In Fig. 2(a), we compare the exact (open circles) and approximate (solid curve) solutions when $\tau$=1 ns and thermo-optic effects are negligible. A good agreement is observed in this case because $\alpha\xi_r/\beta^2 \gg 1 (\approx 26)$. A detailed analysis shows that Eqs. (7) provide an accurate approximation to Eqs. (11) as long as $4\alpha\xi_r \gtrsim \beta^2$. Note that the shape of the bistability curve and the hysteresis loop are quite different for a ring resonator as compared to a Fabry–Perot resonator. Indeed, they exhibit features similar to those observed for bistability during reflection from a nonlinear medium.

The bistable behavior of silicon ring resonators depends dramatically on the operating wavelength λ. As illustrated by Fig. 2(b), a decrease in λ from 1550 to 1547 nm nearly triples the hysteresis width, but a further reduction of λ down to 1544 nm results in a collapse of the bistability phenomenon. This situation also differs from that of a Fabry–Perot resonator, where the variation of operating wavelength does not change the situation qualitatively. The dependence of input–output characteristics on λ and parameters $L_1$, $L_2$, $R$, $\tau$, and $r$ provides multiple tuning knobs for observing bistable behavior in silicon ring resonators and ensures their wide applicability.

It is also possible to realize electronically assisted optical switching at a fixed input intensity by varying free-carrier lifetime with the help of a reverse-biased p–n junction. This possibility is illustrated in Fig. 2(c). If the system is initially in the state $a$ for $I_{\text{in}} \approx 6$ GW/cm$^2$, then changing $\tau$ from $1.2 \rightarrow 1 \rightarrow 1.2$ ns will switch the system up to state $d$ through the transition path $a \rightarrow b \rightarrow c \rightarrow d$. Similarly, changing $\tau$ from $1.2 \rightarrow 1.5 \rightarrow 1.2$ ns will switch the system down from $d$ to $a$ through the path $d \rightarrow e \rightarrow f \rightarrow a$.

Finally, we consider the impact of the TOE. Figure 2(d) shows $I_{\text{tr}}$ as a function of $I_{\text{in}}$ in the presence of TOE using values for the parameters $\kappa$, $\theta$, $C$, and $\rho$ from [6] (the unstable branches are plotted by dotted curves). Inclusion of the TOE results in optical multistability and a reduced switching intensity, but only at the expense of a much lower on–off contrast. It is worth noting that the effect of FCA-induced saturation of the transmitted intensity is common to both ring resonators [see Figs. 2(a)–2(d)] and Fabry–Perot cavities [8].

To summarize, we have presented an analytical model of the nonlinear phenomenon of optical bistability in SOI waveguide ring resonators operating in the cw regime. We outlined the bistable features of ring resonators and compared their bistable behaviors with those of Fabry–Perot cavities. Our analytical results may prove useful in the design and optimization of silicon-based optical memories.

This work was supported by the Australian Research Council through its Discovery Grant scheme under grant DP0877232. The work of G. P. Agrawal is also supported by the National Science Foundation (NSF) award ECCS-0801772.

## References

1. B. Jalali, V. Raghunathan, D. Dimitropoulos, and O. Boyraz, IEEE J. Sel. Top. Quantum Electron. **12**, 412 (2006).
2. Q. Lin, O. J. Painter, and G. P. Agrawal, Opt. Express **15**, 16604 (2007).
3. H. J. Eichler, T. Brand, M. Glotz, and B. Smandek, Phys. Status Solidi B **150**, 705 (1988).
4. V. R. Almeida and M. Lipson, Opt. Lett. **29**, 2387 (2004).
5. G. Priem, P. Dumon, W. Bogaerts, D. V. Thourhout, G. Morthier, and R. Baets, Opt. Express **13**, 9623 (2005).
6. Q. Xu and M. Lipson, Opt. Lett. **31**, 341 (2006).
7. Q. Xu and M. Lipson, Opt. Express **15**, 924 (2007).
8. I. D. Rukhlenko, M. Premaratne, and G. P. Agrawal, Opt. Express **17**, 22124 (2009).
9. X. Chen, N. C. Panoiu, and R. M. Osgood, Int. J. Quantum Chem. **42**, 160 (2006).
10. I. D. Rukhlenko, M. Premaratne, C. Dissanayake, and G. P. Agrawal, Opt. Lett. **34**, 536 (2009).
11. G. P. Agrawal, *Applications of Nonlinear Fiber Optics*, 2nd ed. (Academic, 2008).